



# Hydrothermal Synthesis, Structural Analysis and Photoluminescence Study of Nd<sup>3+</sup>/Ho<sup>3+</sup> Doped Nanophosphors

GIRIJA VENKATESWARA KONERU<sup>1</sup>, VENKATA NAGENDRA KUMAR PUTTA<sup>1\*</sup>  
and SIRISHA BANDI<sup>1,2</sup>

<sup>1</sup>Department of Chemistry, GITAM Deemed to be University, Rudraram, Hyderabad-502329, India.

<sup>2</sup>B. V. Raju Institute of Technology, Narsapur, 502313, Telangana, India.

\*Corresponding author E-mail: pvenkatanagendrakumar@gmail.com, vputta@gitam.edu

<http://dx.doi.org/10.13005/ojc/400106>

(Received: December 18, 2023; Accepted: February 09, 2024)

## ABSTRACT

Through photoluminescence (PL) investigations, this work shows that the hydrothermal technique of nanomaterial synthesis can successfully produce GdPO<sub>4</sub>:Nd<sup>3+</sup>/Ho<sup>3+</sup> nanophosphors that display luminescence properties. Down-conversion peaks that produce green and red light arise at certain wavelengths (465, 550, and 674 nm) in response to stimulation at 300 nm. The analysis indicates the P-O CT band of Ho<sup>3+</sup> ions and non-radiative resonance energy transfer, which boosts Ho<sup>3+</sup> ion emission. GdPO<sub>4</sub>:Nd<sup>3+</sup>/Ho<sup>3+</sup>, an up-conversion (UC) nanophosphor, exhibits efficient luminescence output, with Ho<sup>3+</sup> ions being attributed to distinct peaks in the up-conversion emission spectra (465 nm, 550 nm, and 674 nm). Nd<sup>3+</sup> ions under strong 808 nm laser irradiation promote these peaks. The study produces well-crystalline nanoparticles with diameters ranging from a few nanometers to tens of nanometers by using the hydrothermal synthesis approach. Under PLE tests, the nanophosphors show an impressive quantum yield, suggesting a wide range of possible uses in the field of nanophosphor materials.

**Keywords:** Hydrothermal synthesis, Neodymium ion, Holmium ion, Gadolinium ion, Photoluminescence.

## INTRODUCTION

In the field of materials science, rare earth elements (RE) have attracted a lot of attention because of their easy manufacturing processes and wide range of uses. Temperature sensors, spectrum converters, solar cells, medicinal applications, high-tech enterprises, and other fields have all made extensive use of the integration of RE-doped

nanomaterials. Standardised processes for the large-scale synthesis of dual-mode nanomaterials are yet unattainable, despite their great potential. Rare earth orthophosphates are unique among RE compounds in that they exhibit exceptional thermal stability and chemical resistance, withstanding temperatures as high as 2200°C<sup>1-5</sup>. These materials also have visually pleasing properties, low solubility, and are widely acknowledged as excellent hosts for



radioactive waste adsorption. This work presents a new hydrothermal synthesis technique for producing  $\text{GdPO}_4:\text{Nd}^{3+}/\text{Ho}^{3+}$  dual-mode conversion nanomaterials. When stimulated by a continuous wave (CW) laser, the luminous features of the synthesised material are enhanced due to the precise control of size and shape achieved by this process.  $\text{GdPO}_4$  nanoparticles exhibit both up-conversion (UC) and down-conversion (DC) characteristics, making them an effective luminescence host. Permitted transitions, such as the 300 nm light-absorbing charge transfer (CT) process from  $\text{O}^{2-}$  to  $\text{Gd}^{3+}$ , are responsible for this dual-mode behaviour. When excited by UV radiation, the emission spectra show distinct peaks at around 465 nm, 550 nm, and 674 nm that correspond to  $\text{Ho}^{3+}$  ions, suggesting that down-conversion has occurred. In addition,  $\text{Nd}^{3+}$  acts as a sensitizer by increasing the material's emission intensity of  $\text{Ho}^{3+}$  ions. The upconversion emission spectra of room temperature  $\text{GdPO}_4$  shows emissions from both  $\text{Ho}^{3+}$  and  $\text{Nd}^{3+}$  under near-infrared (IR) light at 808 nm<sup>6-10</sup>. By using an 808 nm laser to excite the sample, it is possible to analyse down-conversion, up-conversion, and energy transfer efficiency processes in detail. These nanomaterials' activated functional groups provide fascinating sensing properties that increase their potential use in a variety of applications, such as bio imaging, security, and optical and display systems<sup>11-14</sup>. Thus, our study adds to the growing body of knowledge on RE-based nanomaterials with customised dual-mode luminous characteristics. From previous synthesis, activation, and characterisation of upconversion crystals doped with  $\text{Yb}^{3+}$  and  $\text{Ho}^{3+}$  are covered in brief in this study<sup>37</sup>. The difficulties and developments in nanotechnology for use in biomedical applications, with an emphasis on the creation of an innovative, very sensitive luminous nano thermometer that has been verified for bio safety<sup>38</sup>. The crystals' surface modification with hydrophilic dextran improves their applicability for cell fluorescence imaging applications, and they exhibit promising upconversion fluorescence features. Results in the literature show that different applications and in the present study  $\text{GdPO}_4:\text{Nd}^{3+}/\text{Ho}^{3+}$  photoluminescent materials are attractive options for many technological and biological applications because of their dual-mode luminescence, tunability, efficient energy transfer, and carefully regulated synthesis.

## Chemical Substances and the Process of Synthesis

**Chemicals Used:** Reactants for the synthesis process were highly pure analytical grade reagents. Among these was Hydrated Gadolinium (III) acetate ( $\text{Gd}(\text{ac})_3 \cdot \text{XH}_2\text{O}$ ), Hydrated Holmium (III) Acetate ( $\text{Ho}(\text{ac})_3 \cdot \text{XH}_2\text{O}$ ), Ammonium Dihydrogen Phosphate ( $(\text{NH}_4)_2\text{H}_2\text{PO}_4$ ), Hydrated Neodymium(III) Acetate ( $\text{Nd}(\text{ac})_3 \cdot \text{XH}_2\text{O}$ ), polyol ethylene glycol (6000), diluted sodium hydroxide (NaOH), concentrated hydrochloric acid (HCl), and deionized water.

## GdPO<sub>4</sub> Synthesis: Ho<sup>3+</sup>/Nd<sup>3+</sup> Nanoparticles

The hydrothermal procedure was adopted to prepare the sample.

### Synthesis Methodology:

$\text{Nd}^{3+}/\text{Ho}^{3+}$  doped  $\text{GdPO}_4$  by hydrothermal synthesis was made to create the nanoparticles. The following is how the sample was made:  $\text{GdPO}_4$  luminous nanoparticles ( $\text{GdPO}_4:\text{Ho}^{3+}, \text{Nd}^{3+}$ ) with 1%  $\text{Ho}^{3+}$  and 20%  $\text{Nd}^{3+}$  were created by doping  $\text{GdPO}_4$  with  $\text{Ho}^{3+}$ . The hydrothermal technique was employed in the synthesis of this compound. In a traditional synthesis, 5 mL of concentrated HCl was mixed with 730.76 mg of  $(\text{CH}_3\text{CO}_2)_3\text{Gd} \cdot \text{XH}_2\text{O}$ , 8.7 mg of  $(\text{CH}_3\text{CO}_2)_3\text{Ho} \cdot \text{XH}_2\text{O}$ , and 178.48 mg of  $(\text{CH}_3\text{CO}_2)_3\text{Nd} \cdot \text{XH}_2\text{O}$ . The mixture was then heated until the materials were dissolved. As a consequence, metal ions were dissolved and formed a clear, transparent solution. 10 mL of deionized water was alternatively added, heated to 80°C at least five times, and the evaporation procedure was repeated in order to eliminate any remaining HCl. There were 298.2 mg of  $(\text{NH}_4)_2\text{HPO}_4$  dissolved in 10 mL of deionized water. Drop by drop, 2.64 g of dissolved NaOH was added to 10 mL of deionized water until the  $(\text{NH}_4)_2\text{HPO}_4$  solution became translucent, resulting in a transparent solution<sup>15-20</sup>. Next, 20 millilitres of PEG(6000) were added to the evaporated metal ion solution, which had been transferred to a 100 millilitre round-bottom flask. At 80°C, it was refluxed for a minimum of 10 min before the  $(\text{NH}_4)_2\text{HPO}_4$  solution was added dropwise. A faint yellow colour was seen when the  $(\text{NH}_4)_2\text{HPO}_4$  solution was added; however, after two hours of heating at 120°C, the colour became white. This suggested that a white precipitate was forming. After allowing the mixture to cool to ambient temperature, it was centrifuged for five minutes at 5000 rpm, twice washed with 10 mL of acetone, then dried under

an infrared light to extract the white powder. The prepared sample was then heated for four hours at 900°C. By Hydrothermal-mediated synthesis technique with PEG (6000), a  $\text{GdPO}_4:\text{Nd}^{3+}/\text{Ho}^{3+}$  nanophosphor compound with a well-defined product morphology was synthesised from Figure 1.

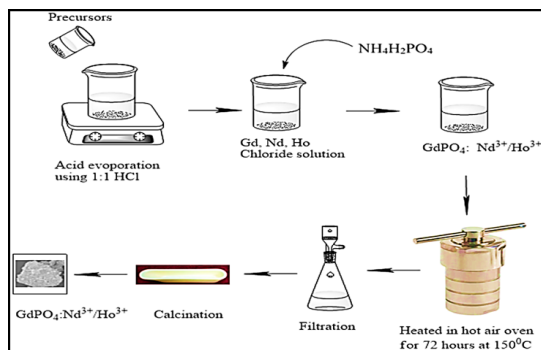


Fig. 1. Schematic Representation of Synthesis of  $\text{GdPO}_4:\text{Ho}/\text{Nd}$

## RESULT AND DISCUSSION

**XRD Analysis:** Fig. 2. XRD analysis can elucidate the successful incorporation of dopants, such as Nd and Ho, into the crystal lattice. Alterations in the diffraction pattern or shifts in peak positions serve as indicators of the presence of dopant ions and their impact on the crystal structure. Additionally, XRD is a valuable tool for evaluating the phase purity of the material<sup>21-25</sup>. The emergence of distinct peaks or the absence of anticipated peaks may hint at the occurrence of impurities or the existence of multiple phases. In cases where a monoclinic phase transformation takes place, XRD typically reveals sharp peaks associated with this structural change. As a result, the XRD pattern of  $\text{GdPO}_4:\text{Ho}/\text{Nd}$  shows distinct peaks at 20 and 35 degrees, which are compatible with the material having a monoclinic crystal structure and matching up with certain crystallographic planes. Because the crystal lattice is non-orthogonal, the Miller indices -101, 210, and -112 indicate a collection of crystallographic planes in a monoclinic structure, with particular intercepts along the a, b, and c axes.

**SEM Analysis:** To summarise, the SEM picture presented in Fig. 3. offers important insights into the morphology of the  $\text{GdPO}_4:\text{Ho}^{3+}/\text{Nd}^{3+}$  nanophosphor material that was annealed at 900°C. It also shows a wide variety of nanoparticle morphologies<sup>26-30</sup>. By displaying the elemental distribution within the nanoparticles, the corresponding compositional

images in Fig. 3 improve comprehension even more and facilitate the interpretation of the material's structural and chemical properties.

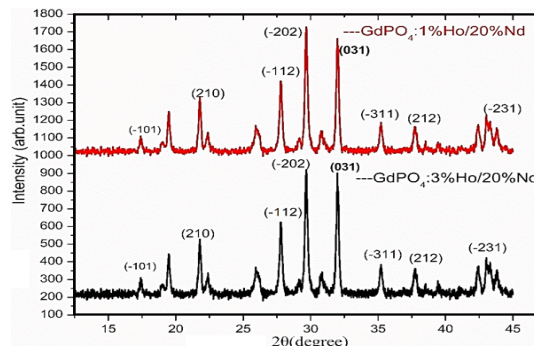


Fig. 2. XRD Analysis of  $\text{GdPO}_4:\text{Ho}/\text{Nd}$

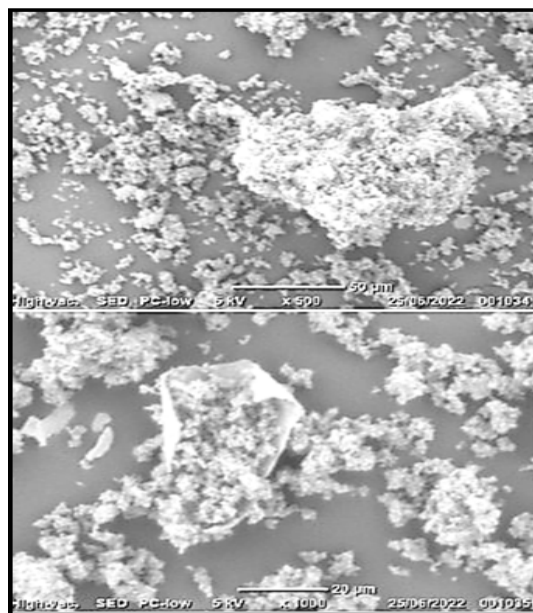


Fig. 3. Representation SEM Analysis of  $\text{GdPO}_4:\text{Ho}/\text{Nd}$

**FT-IR Analysis:** Fig. 4. Since  $\text{GdPO}_4$  is intrinsically a phosphate-based compound, its FT-IR spectra doped with  $\text{Nd}^{3+}$  and  $\text{Ho}^{3+}$  should exhibit characteristic vibrations linked to the phosphate ( $\text{PO}_4^{3-}$ ) groups. Specifically, it is expected that the phosphate groups' symmetric stretching vibrations will appear as a significant peak between 1000 and 1200  $\text{cm}^{-1}$  wavenumber range. The FT-IR spectra provide a comprehensive tool for clarifying different vibrational features of the dopants, spanning a wide range from 4000  $\text{cm}^{-1}$  down to about 400  $\text{cm}^{-1}$ . Various portions of the spectrum shed light on the distinct vibrational modes and interactions found in the doped  $\text{GdPO}_4$ , giving rise to a thorough

comprehension of its molecular makeup and bonding arrangements. In the end, the presence of certain vibrational modes, maybe connected to O-H stretching vibrations or metal-oxygen bonding, is suggested by the peak at  $4400\text{ cm}^{-1}$  in the FT-IR spectra of  $\text{GdPO}_4$  doped with Ho and Nd.

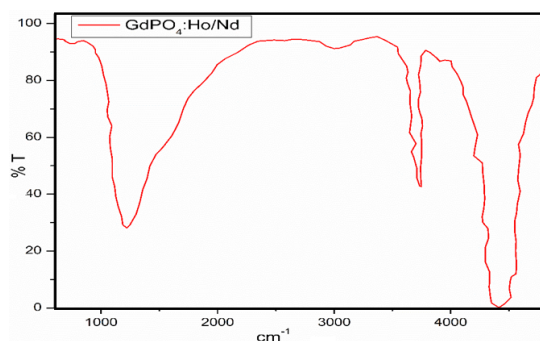


Fig. 4. FT-IR Analysis of  $\text{GdPO}_4\text{:Ho/Nd}$

### PL Studies

Studies on photoluminescence (PL) examine how a material emits light (photons) in response to external light sources, usually visible or ultraviolet (UV) light. PL studies in the Fig. 5. of  $\text{GdPO}_4\text{:Ho/Nd}$  nanophosphors concentrate on comprehending the material's luminescent characteristics, particularly the emission of light at particular wavelengths. The PL spectrum exhibits peaks at 465 nm, 550 nm, and 674 nm that reveal important details about the energy levels and electronic transitions of the dopant ions ( $\text{Ho}^{3+}$  and potentially  $\text{Nd}^{3+}$ ).

### A Explanation of PL studies is provided below Electron Excitation

The material is first exposed to a light source, usually UV or Visible light, in photoluminescence (PL) studies. Higher energy levels are excited in the material's electrons by this external energy.

### Elevations of Energy and Electronic Changes

After being raised to higher energy levels, the excited electrons eventually descend back to their ground state. They release photons, which are units of energy, during this process. The energy differences between various electronic states are indicated by the particular wavelengths at which photons are emitted.

### $\text{Ho}^{3+}$ Ions

The observed luminescence may be caused by 808 laser excited yet 300 nm certain electronic

transitions occurring within the  $\text{Ho}^{3+}$  ions, as indicated by the peaks at 465, 550, and 674 nm. Every peak represents a distinct transition in energy levels, and these transitions are frequently connected to the distinctive electronic structure of  $\text{Ho}^{3+}$ .

### Influence of $\text{Nd}^{3+}$

It is necessary to take into account the impact of any  $\text{Nd}^{3+}$  dopant ions on the PL spectrum. Changes in energy levels and emission characteristics may result from interactions between  $\text{Nd}^{3+}$  and  $\text{Ho}^{3+}$  ions as well as from their interactions with the host lattice  $\text{GdPO}_4$ .

### Peak at 465 nm

One possible explanation for a peak in the photoluminescence spectra at 465 nm is that it corresponds to an energy level or electronic transition in the  $\text{Ho}^{3+}$  ions. Rare-earth ion electronic transitions frequently cause emission peaks in the visible spectrum. One way to determine the precise transition causing this peak is to compare it with known energy levels of  $\text{Ho}^{3+}$  in the literature and do more research.

### Peak at 550 nm

It is possible that another electronic transition within the  $\text{Ho}^{3+}$  ions is responsible for the peak at 550 nm. In the visible spectrum, distinctive emission peaks are caused by the energy difference between the various electronic states of rare-earth ions. Understanding the nature of this luminescence can be gained by reviewing the literature on  $\text{Ho}^{3+}$  transitions in comparable to host materials.

### Peak at 674 nm

In a similar way, the signal at 674 nm indicates that the  $\text{Ho}^{3+}$  ions may undergo one more electronic transition. The literature contains extensive information on the energy levels and transitions of rare-earth ions, and comparing the measured peaks with known transitions can aid in deciphering the material's luminous characteristics.

Not to be ignored there is a possibility that the presence of  $\text{Nd}^{3+}$  dopant ions will also affect the material's overall photoluminescence behaviour<sup>31-36</sup>. Changes in energy levels and emission characteristics can result from the interaction between dopants and the host lattice. Literature sources discussing PL studies on

GdPO<sub>4</sub>:Ho/Nd nanophosphors, particularly those focusing on emission peaks around 465 nm, 550 nm, and 674 nm, would provide a more detailed and specific explanation.

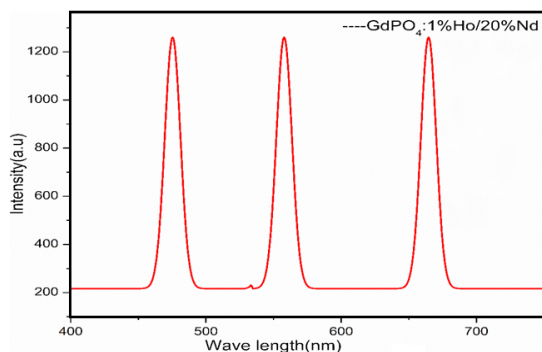


Fig. 5. PLE Studies of GdPO<sub>4</sub>:Ho/Nd

### CONCLUSION

Finally, this work greatly contributes to our understanding of GdPO<sub>4</sub>:Nd<sup>3+</sup>/Ho<sup>3+</sup> nanomaterials.

Together, the morphological information from SEM, the XRD confirmation of dopant incorporation, and the information from FT-IR allow for a thorough characterisation. The photoluminescence experiments' observed electronic changes highlight the potential uses of these nanomaterials across a range of technological and biological fields. This discovery not only opens up new avenues for future research, but it also offers insightful information on the structural and optical characteristics.

### ACKNOWLEDGMENT

My heartfelt appreciation goes to GITAM Deemed to be University (Hyderabad) for providing a facility for synthesis.

### Conflicts of interest

We have no competing interests that could Influence our research or findings.

### REFERENCES

- Bhonsule, S. U.; Wankhede, S. P.; & Moharil, S.V., *In AIP Conference Proceedings.*, **2018**, *1953*, 1.
- Perala, R. S.; Singh, B. P.; Putta, V. N. K.; Acharya, R.; & Ningthoujam, R. S., *ACS omega.*, **2021**, *6*, 19517-19528.
- Perala, R. S.; Joshi, R.; Singh, B. P.; Putta, V. N. K.; Acharya, R.; & Ningthoujam, R. S., *ACS omega.*, **2021**, *6*, 19471-19483.
- Szczygieł, I.; Macalik, L.; Radomska, E.; Znamierowska, T.; Moczka, M.; Godlewska, P.; & Hanuza, J., *Optical Materials.*, **2007**, *29*, 1192-1205.
- Kumar, V.; & Wang, G., *Journal of Luminescence.*, **2018**, *199*, 188-193.
- Parchur, A.K.; Ningthoujam, R.S., *RSC Advances.*, **2012**, *2*, 10854-10858.
- Niu, C.; Li, L.; Li, X.; Lv, Y.; Lang, X., *Optical Materials.*, **2018**, *75*, 68-73.
- Yu, C.; Yu, M.; Li, C.; Liu, X.; Yang, J.; Yang, P.; & Lin, J., *Journal of Solid State Chemistry.*, **2009**, *182*, 339-347.
- Prorok, K.; Bednarkiewicz, A.; Cichy, B.; Gnach, A.; Misiak, M.; Sobczyk, M.; Strek, W., *Nanoscale.*, **2014**, *6*, 1855-1864.
- AitMellal, O.; Oufni, L.; Messous, M. Y.; Trandafir, M. M.; Chirica, I. M.; Florea, M.; Nea u, F., *Journal of Solid State Chemistry.*, **2021**, *301*, 122310.
- Wang, G.; Peng, Q.; Li, Y., *Accounts of Chemical Research.*, **2021**, *44*, 322-332.
- Kang, X.; Li, C.; Cheng, Z.; Ma, P. A.; Hou, Z.; Lin, J., *Wiley Interdisciplinary Reviews: Nano Medicine and Nano Biotechnology.*, **2014**, *6*, 80-101.
- Kumar, V.; Rani, P.; Singh, D.; Chawla, S., *RSC Advances.*, **2014**, *4*, 36101-36105.
- Suryawanshi, I.; Srinidhi, S.; Singh, S.; Kalia, R.; Kunchala, R. K.; Mudavath, S. L.; Naidu, B.S., *Materials Today Communications.*, **2021**, *26*, 102144.
- AitMellal, O.; Oufni, L.; Messous, M. Y.; Trandafir, M. M.; Chirica, I. M.; Florea, M.; Nea u, F., *Journal of Solid State Chemistry.*, **2021**, *301*, 122310.
- Tyminski, A.; Smiechowicz, E.; Martín, I.R.; Grzyb, T., *ACS Applied Nano Materials.*, **2020**, *3*, 6541-6551.
- Lyu, T.; Dorenbos, P., *Journal of Materials Chemistry C.*, **2018**, *6*, 369-379.
- Gavrilovi, T.; Periša, J.; Papan, J.; Vukovi, K.; Smits, K.; Jovanovi, D. J.; Dramićanin, M. D., *Journal of Luminescence.*, **2018**, *195*, 420-429.
- Hu, F.; Wei, X.; Qin, Y.; Jiang, S.; Li, X.; Zhou, S.; Yin, M., *Journal of Alloys and Compounds.*, **2016**, *674*, 162-167.

20. Thakur, H.; Singh, B.P.; Kumar, R.; Gathania, A.K.; Singh, S.K.; Singh, R.K., *Materials Chemistry and Physics.*, **2020**, *253*, 123333.
21. Frost, R.; Hales, M.; Martens, W., *Journal of Thermal Analysis and Calorimetry.*, **2009**, *95*, 999-1005.
22. Ren, W.; Tian, G.; Zhou, L.; Yin, W.; Yan, L.; Jin, S.; Zhao, Y., *Nanoscale.*, **2012**, *4*, 3754-3760.
23. Yi, Z.; Lu, W.; Qian, C.; Zeng, T.; Yin, L.; Wang, H.; Zeng, S., *Biomaterials Science.*, **2014**, *2*, 1404-1411.
24. Tadge, P.; Yadav, R. S.; Vishwakarma, P. K.; Rai, S. B.; Chen, T. M.; Sapra, S.; Ray, S., *Journal of Alloys and Compounds.*, **2020**, *821*, 153230.
25. Fang, Y. P.; Xu, A. W.; Song, R. Q.; Zhang, H. X.; You, L. P.; Yu, J. C.; Liu, H. Q., *Journal of the American Chemical Society.*, **2003**, *125*, 16025-16034.
26. Haase, M.; Schäfer, H., *Angewandte Chemie International Edition.*, **2011**, *50*, 5808-5829.
27. Sukul, P.P.; Kumar, K., *Methods and Applications in Fluorescence.*, **2016**, *4*, 044005.
28. Cesaria, M.; DiBartolo, B., *Nanomaterials.*, **2019**, *9*, 1048.
29. Qu, Z.; Shen, J.; Li, Q.; Xu, F.; Wang, F.; Zhang, X.; Fan, C., *Theranostics.*, **2020**, *10*, 2631.
30. Duc-Tin, Q.; Keppler, H., *Contributions to Mineralogy and Petrology.*, **2015**, *169*, 1-26.
31. Hudry, D.; Howard, I.A.; Popescu, R.; Gerthsen, D.; Richards, B.S., *Advanced Materials.*, **2019**, *31*, 1900623.
32. Yada, M., *In Inorganic and Metallic Nano tubular Materials. Springer, Berlin, Heidelberg.*, **2010**, *48*, 97-115.
33. Runowski, M.; Grzyb, T.; Zep, A.; Krzyczkowska, P.; Gorecka, E.; Giersig, M.; Lis, S., *RSC Advances.*, **2014**, *4*, 46305-46312.
34. Bouddouch, A.; Amaterz, E.; Bakiz, B.; Taoufyq, A.; Guinneton, F.; Villain, S.; Benhachemi, A., *Optik.*, **2021**, *238*, 166683.
35. Bandi, S.; Kanuparth, P. R.; & Putta, V. N. K. *Orient. J. Chem.*, **2023**, *39*.
36. Bandi, S.; Kanuparth, P. R.; & Putta, V. N. K. *Asian Journal of Chemistry.*, **2023**, *35*.
37. Li, X.; Zhu, J.; Man, Z.; Ao, Y.; & Chen, H. *Scientific Reports.*, **2014**, *4*, 4446.
38. Sofi, A. H., & Shah, M. A. *Materials Research Express.*, **2014**, *1*, 015041.